Liu, S., Pan, W., Cao, Q., Long, Z., Jiang, Y, and Chen, Q. 2019. "CFD simulations of natural cross ventilation through an apartment with modified hourly wind information from a meteorological station," *Energy and Buildings*, 195: 16-25.

CFD simulations of natural cross ventilation through an apartment with modified hourly wind information from a meteorological station

Sumei Liu[a], Wuxuan Pan[a], Qing Cao[a], Zhengwei Long[a], Yi Jiang[b], Qingyan Chen[c*],
[a]*Tianjin Key Laboratory of Indoor Air Environmental Quality Control, School of Environmental Science and Engineering, Tianjin University, Tianjin, China*
[b]*XIN Center, Tsinghua University, Beijing, China*
[b]*School of Mechanical Engineering, Purdue University, West Lafayette, IN, USA*

HIGHLIGHTS

- Interpolating hour-by-hour wind velocity from a meteorological station into minute-by-minute velocity
- CFD simulations of the outdoor wind velocity around an apartment building and the indoor cross-ventilation rate in an apartment
- Verification of the computed results with corresponding experimental data

ABSTRACT

Natural ventilation in buildings can improve indoor air quality and thermal comfort and reduce air-conditioning use except for highly polluted area. Traditionally, the inflow boundary conditions for calculating natural ventilation used weather data from a meteorological station that is often in a suburb. The use of hour-by-hour wind velocity from the station may give rise to some errors because of the large time step. This investigation proposed a correlation method for converting the hour-by-hour wind velocity from a meteorological station to minute-by-minute velocity, using data measured on the rooftop of the building of interest. A CFD simulation with the coupled modeling method using the unsteady RNG k-ε model was performed to calculate airflow around the building and airflow in an apartment simultaneously. The computed outdoor wind velocity and indoor ventilation rate were compared with the corresponding experimental data. The results showed that the simulations calculated the outdoor wind velocity on the building rooftop and the cross-ventilation rate through the apartment with acceptable accuracy.

Keywords: Unsteady flow, Field measurements, Airflow around building, Meteorological station

1. Introduction

Natural ventilation can improve indoor air quality by 20-47% [1], potentially reduce energy consumption by 8-78% [2], and provide a high level of thermal comfort for occupants [3]. Unfortunately, natural ventilation cannot be used in all climates, since the weather conditions, such as the outdoor air quality and thermal environment, are an important factor [4]. Certainly, places such as Kunming, China, have favorable weather for natural ventilation. Even in these places, however, it is challenging to design natural ventilation because of the effects of opening size and location [5,6], the transient interaction between the indoor and

* Address correspondence to Qingyan Chen, School of Mechanical Engineering, Purdue University, 585 Purdue Mall, West Lafayette, IN 47907, USA. E-mail: yanchen@purdue.edu.

outdoor environment, unsteady wind conditions [7], irregular urban geometry [8], variations in outdoor air quality [2], and so on.

The driving force for natural ventilation is the pressure differential created by wind and thermal buoyancy. Therefore, in the design of naturally ventilated buildings, the first step is to obtain reliable meteorological wind information, such as wind speed and direction [9]. One can then design natural ventilation by various methods, such as the analytical method, (semi-)empirical models, the wind tunnel method, and the computational fluid dynamics (CFD) method.

Natural ventilation can be divided into wind-driven cross ventilation and single-sided ventilation. Wind-driven cross ventilation entails a high flow rate through a building and is more desirable. Therefore, this investigation focused on cross ventilation. Many analytical and (semi-)empirical models have been developed to calculate cross ventilation rate, such as the models proposed by Etheridge and Sandberg [10], Chu and Wang [11], and Aynsley [12]. Among the existing method, analytical and (semi-)empirical models can provide rapid estimates of the cross ventilation rate. Although these models are useful and easy to use, they introduce large uncertainties due to the assumptions used [13]. The wind tunnel method exhibits good control of the inflow boundary conditions [14] but does not vary wind speed and direction over time and is very expensive. Meanwhile, the CFD method can account for major influencing factors. Although CFD is computationally demanding, its accuracy and reliability in determining the ventilation rate make it an ideal tool for cross-ventilation design [15-17].

Previously published CFD models for cross-ventilation simulation can be classified into three types, the decoupled modeling method [18], compact integration modeling method [19], and coupled modeling method [20]. The decoupled modeling method simulates indoor airflow separately by assigning fixed pressure at windows, where the pressure is determined at the building façade with solid building blocks for outdoor airflow simulation [21]. When this method is used, the computing time and capacity are minimal. However, this simple method predicts that airflow enters the exterior windows of an apartment perpendicularly, which is unrealistic and inaccurate. The compact integration modeling method first calculates outdoor airflow with solid building blocks. The method then simulates airflow through and around an apartment in a building with the use of flow information extracted at a certain distance from the building in the outdoor airflow simulation [19]. However, the specified distance from the building has an impact on the calculated cross-ventilation rate. The coupled modeling method calculates outdoor wind flow and indoor natural ventilation simultaneously [22]. This method can capture the complex interaction between outdoor wind flow and indoor natural ventilation, and thus it is the most accurate. Unfortunately, the coupled modeling method is the most computationally demanding.

Nevertheless, a number of researchers have adopted the coupled modeling method to investigate cross ventilation. Some researchers have focused on an isolated or generic building [23-25]. To take into account the influence of surrounding buildings on the airflow around the building of interest, other researchers have considered the sheltering effect of neighbouring buildings on the indoor air flow [26-28]. Several investigations have explored the indoor cross-ventilation rate using actual urban configurations [8,29], but doing so requires detailed information about urban geometry. It should be noted that all these investigations used hourly wind velocity and direction obtained from a meteorological station as inflow boundary conditions. This was because a meteorological station typically provides hourly data. In reality, cross ventilation should be determined minute by minute or even second by second. Our earlier studies [30,31] found that, although the hourly wind velocity and direction from a meteorological station may have been the same at two different moments in time, the wind speed measured on a building rooftop varied considerably. Should

CFD be used to calculate the wind speed on the rooftop, the results would be the same for the two moments. This is because CFD simulation using hourly wind data cannot account for wind extremes and variations that occur within a given hour.

Thus, appropriate wind information within an hour-long period is prerequisite for obtaining rational wind flow fields, and subsequently the cross-ventilation rate, by means of CFD. Although wind may vary significantly within an hour, hourly meteorological data does not contain this information. Previous studies have not correctly considered the transient characteristics of wind. To fill this gap, the present investigation proposed the use of a correlation method to convert hourly wind data from a meteorological station to minute-by-minute or even second-by-second transient data. The method enabled us to take the unsteady character of the inflow boundary into account and thus maintain the accuracy of the simulation results.

2. Research Method

This section describes a correlation method for converting hour-by-hour meteorological data from a meteorological station into minute-by-minute data. We then discuss the experimental approach for obtaining wind velocity on a building rooftop and the indoor cross-ventilation rate in order to validate the method. Finally, this section illustrates the numerical procedure for computing the cross-ventilation flow.

2.1 Correlation method for obtaining minute-by-minute wind velocity

Traditionally, the inflow boundary conditions for calculating natural ventilation have used hourly weather data from a meteorological station that is often located in a suburb. The large time interval contributes significant error to the calculated rate because the wind can change significantly within an hour. Our previous studies [30,31] found that, although the hourly wind velocity and wind direction from the meteorological station may have remained the same within a given period, the wind measured on a building rooftop varied considerably. We suspect that the wind extremes and variations during the period could be the cause of the variation.

To verify the above hypothesis, the ideal approach would be to obtain more detailed wind information from a meteorological station. Unfortunately, the finest time interval in the data provided by a station is one hour. However, a study by Robaa [32] found a very strong correlation between wind information from a meteorological station and that from a local weather station within the city, as shown in Figure 1.

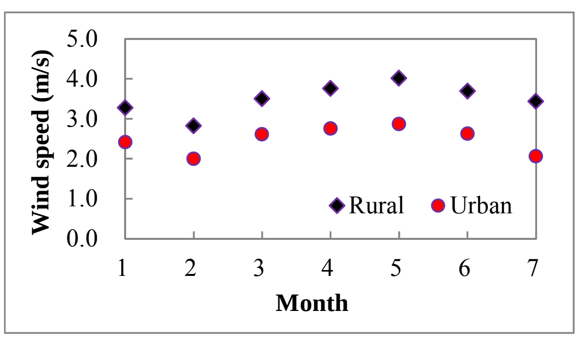

Fig. 1. Comparison of mean wind speed in rural and urban areas [32].

In addition, the ASHRAE Handbook of Fundamentals [33] provides a correlation equation linking local wind speed on a building rooftop, terrain type, building height, and wind speed from a meteorological station as follows:

$$U_H = U_{met}\left(\frac{\delta_{met}}{H_{met}}\right)^{\alpha_{met}}\left(\frac{H}{\delta}\right)^{\alpha} \tag{1}$$

where U_H (m/s) is the local wind speed on the rooftop, H (m) the building height, and U_{met} (m/s) the wind speed from a meteorological station. The coefficients α and α_{met} and the thickness of boundary layer δ in Eq. (1) are related to terrain type [33].

Although there is heat island effect in urban area, its impact on wind flow is minimum. Thus, almost all studies on cross-ventilation assumed isothermal conditions [13,16,34] since buoyancy force is much smaller compared with inertial force from wind. Thus, we can use Eq. (1) to determine U_{met} from measured U_H because the relationship is linear. If U_H contains extremes and large variations within one hour, U_{met} must have the same behavior. Meanwhile, Eq. (1) can also be applied to the average wind velocity in one hour:

$$U_{ave} = U_{met,ave}\left(\frac{\delta_{met}}{H_{met}}\right)^{\alpha_{met}}\left(\frac{H}{\delta}\right)^{\alpha} \tag{2}$$

By combining Eqs. (1) and (2), we obtain

$$U_t/U_{ave} = U_{met,t}/U_{met.ave} \qquad t = 1, \dots, 60\ min \tag{3}$$

If we consider U_t and $U_{met,t}$ as minute-by-minute wind velocity, $U_{met,t}$ can be obtained from U_t according to Eq. (3). Since the minute-by-minute wind information has a sufficiently small time interval, it should contain wind extremes and large variations. Note that we only considered the relationship between the wind speed at a meteorological station and that on a building rooftop. Therefore, this method has been verified only for those cases in which wind direction is relatively stable during the period concerned.

2.2 Validation method for the correlation via field measurements of wind velocity

With the $U_{met,t}$ from Eq. (3), one can use the coupled modeling method to determine the natural ventilation rate through an apartment for a period of time. If the measured cross-natural-ventilation rate is the same as the calculated rate, then the correlation method has been indirectly validated as reliable and accurate.

This investigation measured the wind velocity on a building rooftop and the cross-natural-ventilation rate through an apartment in Tianjin, China. Figure 2(a) shows the apartment building with a weather station P1 on the rooftop. The cross-ventilation rate was measured in a two-bedroom apartment on the third floor of the building. Figure 2(b) shows the floor plan of the apartment. Since our objective was to measure cross ventilation in the apartment, we artificially created a cross-ventilation passage inside the apartment as enclosed by the red lines in the figure. This passage was achieved by closing the hallway to the living room. Except for the south window, north window and interior doors that were open, all external windows were closed. Therefore, cross ventilation could occur only through the south and north windows. The opening of the south window was 0.15 m wide and 1.2 m high, and that of the north window was 0.15 m wide and 1.3 m high.

(a) (b)

Fig. 2. (a) A weather station installed on the rooftop of an apartment building and (b) the floor plan of the apartment where cross-ventilation rate was measured.

This investigation used a HOBO micro weather station to measure the rooftop wind velocity and direction from March 8, 2018, to May 7, 2018. The measurement location was 2 m above the roof of the apartment building, as shown in Figure 2(a). The measuring frequency was one minute. The micro weather station had a measuring accuracy of ±0.4% for wind speed if it was greater than 0.5 m/s, and ±5° for wind direction. The measured wind data can be used to convert the wind from the meteorological station in a Tianjin suburb to minute-by-minute data and to validate the simulated outdoor wind environment around the building.

To measure the cross-ventilation rate, this investigation used the tracer-gas-concentration decay method. Carbon dioxide was used as the tracer gas. Strictly, to obtain reliable results for the air change rate in an enclosure using the tracer-gas technique, the tracer gas should be uniformly mixed in the enclosure. However, complete mixing is difficult to achieve in a real building because of the complexity of the building’s interior layout. Moreover, cross ventilation in the apartment involved four separated zones connected by three interior doors as shown in Figure 2(b), which further increased the complexity. According to Charlesworth [35], one can overcome this problem by measuring the tracer-gas concentration at several locations. The mean of these concentrations can then be assumed to be the average concentration in the entire enclosure. Therefore, this investigation measured the CO_2 concentration at five different locations, shown as P1 to P5 in Figure 2(b). Carbon dioxide was first released in each room, and two portable fans and one air-conditioning unit in ventilation mode were used to mix the CO_2 with the room air. When the CO_2 concentration at all five measuring locations reached about 5000 ppm, the CO_2 injection, the fans, and the air-conditioning unit were all switched off. The south and north windows were then opened, while the CO_2 concentrations at the five locations were continuously measured until the concentration reached 500 ppm. The measurements lasted from 30 to 90 minutes, depending on the outdoor airflow conditions. The tracer-gas-decay method was used to calculate the corresponding ventilation rate from the CO_2 concentrations [36].

2.3 Numerical procedure for computing cross-ventilation flow

2.3.1 Brief description of turbulence model

This investigation used a commercial CFD program, ANSYS Fluent 14.0 [37], to conduct the coupled modeling. The modeling used the unsteady Reynolds-averaged Navier-Stokes

(RANS) equations with the RNG k-ε turbulence model [38] to solve the turbulent wind flow in the computational domain. The model has performed well in simulating urban wind flows [29]. The governing transport equations were solved by using the finite volume method. The species equation was utilized to calculate the transient decay of the CO_2 concentration. The numerical method used the SIMPLE algorithm for coupling pressure and velocity equations, and the second-order discretization schemes for the convection and viscous terms of the governing equations. The modeling used the second-order implicit time integration for temporal discretization with a time step of 30 s. Van Hooff and Blocken [29] compared three different time-step sizes (Δt = 5 s, 10 s and 30 s) and found that the time-step size had no noticeable effect on the scaled residuals. In the present study, the results were considered converged when the residuals for all the independent parameters reached 10^{-4} at the end of each time step. For more detailed information about the numerical technique, please refer to the program manual [36]. In addition, this investigation compared steady and un-steady RANS simulations.

2.3.2 Geometrical model

Our previous study [31] proposed a full-scale model which can be used to calculate the wind flow around a building by using wind information from the nearest meteorological station. To achieve acceptable results, a CFD simulation should incorporate detailed structures around the building within a radius of at least three times the length scale, where the length scale is the maximum dimension of the building. Therefore, we used a full-scale model that extended from the apartment building with surrounding buildings within three length scales to the nearest nearby meteorological station, which was located 10 km away, as shown in Fig. 3(a). The other regions were simplified with different roughness lengths, illustrated in different colors. The computational domain was 12.6 km long, 5.4 km wide and 0.351 km high. Figure 3(b) depicts the buildings within three length scales around the apartment building. Figure 3(c) illustrates the layout of the apartment used in the coupled modeling.

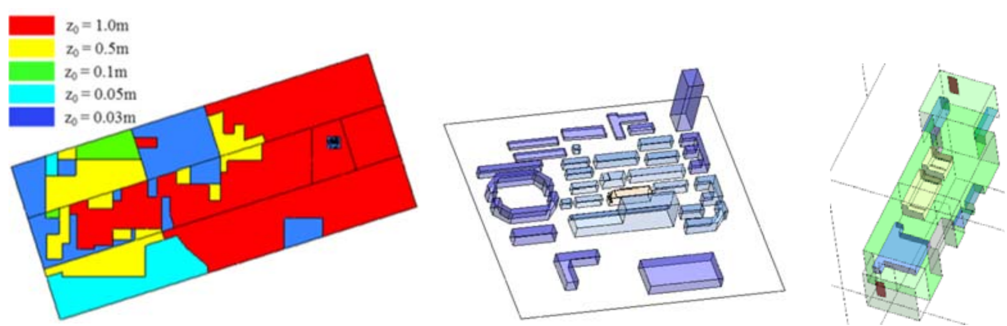

(a) (b) (c)

Fig. 3. Geometric model used in this study: (a) full-scale model with detailed building structures around the apartment building within three length scales and different roughness lengths for the rest of the computational domain, (b) detailed geometry of the apartment building with surrounding buildings within three length scales, and (c) layout of the apartment.

2.3.3 Grid arrangement and mesh generation

Gambit software (version 2.4.6) [39] was used to generate a discrete grid for discretizing the governing transport equations. Because of the complexity of the geometrical model, this study used a hybrid grid scheme with a tetrahedral grid, which can be adapted to various geometric structures. The grid size for the apartment shown in Fig. 3(c) was 0.1 m. The grid size for the domain shown in Fig. 3(b) ranged from 1 to 7 m, and for the remaining area shown in Fig. 3(a) it ranged from 7 to 20 m. The maximum grid size in the vertical direction was 10 m. The resulting total grid number was 4.8 million. Fig. 4(a) depicts the grid cell distribution for the apartment and Fig. 4(b) the distribution around the building. Our previous papers [30,31] show that the grid resolution can lead to grid independent results.

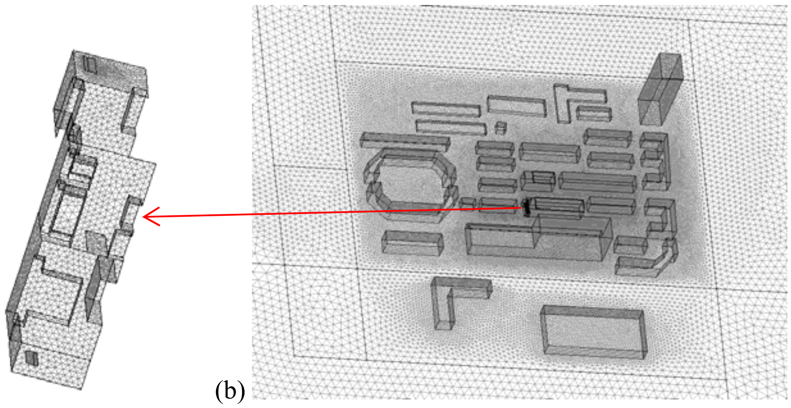

(a) (b)

Fig. 4. Grid cell distribution for (a) the apartment and (b) the building surroundings.

2.3.4 Boundary conditions

The modeling used wind data from a meteorological station in the upwind direction as the inflow boundary conditions. The meteorological station was located 10 km southwest of the apartment building. This investigation selected the time period from 19:00 to 20:00 on April 18, 2018, for modelling the airflow around the building. The corresponding wind angles from the meteorological station at 19:00 and 20:00 were 220° and 219°, respectively, which were from the southwest direction. Thus, the meteorological station was located in upstream of the apartment building. The simulation was able to set vertical western and southern boundaries in the computational domain as inflow. The two downstream vertical boundaries in the computational domain were modeled as outflow. The sky was treated as symmetric. The ground surface was simulated as non-slip conditions with roughness.

The roughness length (z_0) for the ground surface between the meteorological station and the apartment region was determined from sand-grain roughness height k_s and the roughness constant C_s derived by Blocken et al. [41]:

$$k_s C_s = 9.793 z_0 \tag{4}$$

The simulations employed the standard wall function [41, 42] to describe the sand-grain-based roughness. When the k_s and C_s, are varied, Eq. (4) can be used to describe different aerodynamic roughness lengths, z_0, to take into account the influence of roughness elements on the wind flow field. Table 1 lists z_0 values for different terrains and the corresponding k_s and C_s. Figure 3(a) shows the different roughness lengths used for the computational domain.

Table 1.
Roughness for different terrains [40, 43]

Type	**z_0 (m)**	**k_s (m)**	**C_s (m)**
Grassland	0.03	0.5	0.59
Few isolated obstacles	0.05	1.0	0.5

Low crops / Occasional large obstacles	0.1	1.0	1.0
Parkland / Shrubs / Numerous obstacles	0.5	1.0	4.897
Densely distributed mid-rise and high-rise buildings	1.0	1.0	9.793

The wind speed measurements from the meteorological station ($U_{met,ave}$) at 7:00 PM and 8:00 PM were both 1.8 m/s. According to Eq. (3), the correlated minute-by-minute wind speed, $U_{met,t}$, can be used to define the inflow profiles, $U_{z,t}$. The vertical velocity profile for the inflow boundary was modeled as a power law, and the vertical profiles for $k_{z,t}$ and $\varepsilon_{z,t}$ were taken from AIJ guidelines for practical applications of CFD to the pedestrian wind environment around buildings [44], as follows:

$$U_{z,t} = U_{r,t}\left(\frac{z}{z_r}\right)^{\alpha} \tag{5}$$

$$k_{z,t} = (I_{z,t}U_{z,t})^2 \tag{6}$$

$$\varepsilon_{z,t} = U_{ABL,t}^{*^3}/k(z + z_0) \tag{7}$$

where

$$I_{z,t} = 0.1(\frac{z}{z_G})^{(-\alpha-0.05)} \tag{8}$$

$$U_{ABL,t}^{*} = kU_{r,t}/\ln((z_r + z_0)/z_0) \tag{9}$$

The $U_{z,t}$ (m/s) is the minute-by-minute velocity profile (m/s). The $U_{r,t}$ (m/s) in Eq. (5) is the minute-by-minute velocity at reference height z_r (m), and z (m) is height. Because the meteorological station was located in a suburb, the exponent in the power law was α = 0.22 [33] at the two inlet boundaries. The $k_{z,t}$ is the vertical distribution of turbulent energy. The $I_{z,t}$ in Eq. (6) is the minute-by-minute turbulent intensity profile. The $\varepsilon_{z,t}$ is the turbulence dissipation profile. In Eq. (7). U_{ABL}^{*} is the atmospheric boundary layer friction velocity, while k is the Karman constant (= 0.4). The z_G (m) in Eq. (8) is the boundary layer height (= 370 m) determined by terrain category [33].

Note that we conducted both unsteady and steady CFD simulations for airflow around the building. For the unsteady simulation, the profiles for U, k, and □ at the inflow boundaries were provided minute-by-minute. For the steady CFD simulation, the profiles were defined using the average data in that period.

Figure 5 shows the wind rose of Tianjin. The prevailing wind was from south-south-west direction. The annual frequency of our simulated case is 2.2%.

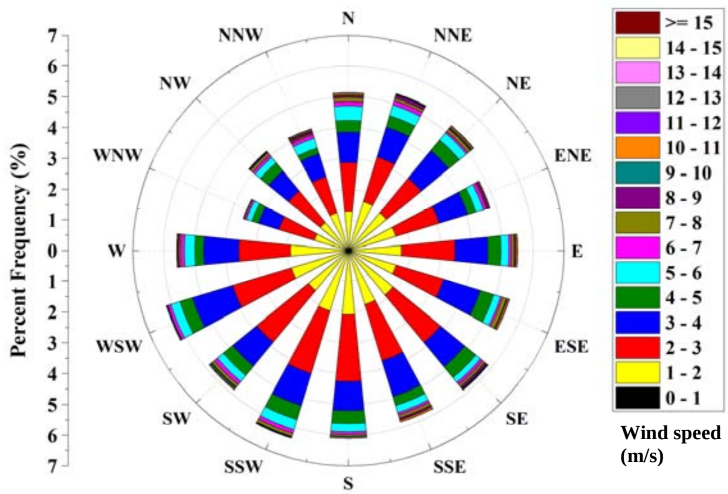

Fig. 5. Wind rose of Tianjin.

3. Results

3.1 Conversion of hourly wind speed to minute-by-minute data

For conversion of hour-by-hour meteorological data from a meteorological station to minute-by-minute data, the wind direction during the period under consideration needs to be relatively stable. Figure 6(a) depicts the wind-direction variation on the rooftop from 19:00 to 20:00 on April 18, 2018, which was stable. According to [45], the average for the first two minutes of an hour can be used to represent the hourly weather data. Therefore, the average wind speed for the first two minutes was used as the denominator in Eq. (3). Figure 6(b) depicts the minute-by-minute wind speed with the wind velocity from the meteorological station and the building rooftop from 19:00 to 20:00. The calculated wind speed was time-dependent and dynamic. Traditional CFD simulations using constant wind speed do not consider the dynamic wind speed, which may cause errors.

(a) 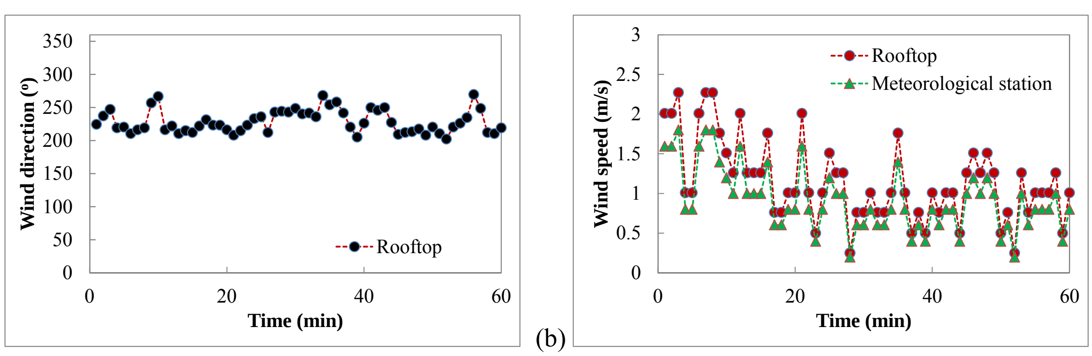

Fig. 6. (a) The measured wind direction on the rooftop of the apartment building, and (b) the converted minute-by-minute wind speed with the wind velocity from the meteorological station and the building rooftop.

3.2 Outdoor wind-speed simulations

This investigation first conducted a steady CFD simulation, which is a popular method of calculating airflow around a building. The simulated wind speed on the building rooftop was 1.73 m/s. When we averaged the measured wind speed on the roof of the apartment building from 19:00 to 19:02, the value was 2.27 m/s. Meanwhile, when we averaged the minute-by-minute wind speed from 19:00 to 20:00, the value was 1.1 m/s. The calculated wind speed did not agree with the two averaged wind speeds from the measurements.

For further analysis of the differences, Figure 7 shows the minute-by-minute wind speed on the building rooftop and the hourly data from the meteorological station from 17:00 to 21:00 on April 18, 2018. The wind speed from the meteorological station decreased from 4.9 m/s to 1.0 m/s during this period. The wind speed on the rooftop exhibited the same trend, but the changes were not proportional. Although the wind speed measurements from the meteorological station at 19:00 and 20:00 were both 1.8 m/s which appear steady, the wind speed on the roof continued to decrease. By using the steady-state numerical simulations with the inflow boundary conditions from the meteorological station at 19:00 and 20:00, the CFD simulation would have produced the same results. Thus, the steady-state simulations seemed problematic. The main reason was that the hourly wind speed from the meteorological station did not represent the wind variation during the two hours. The question, then, was whether transient simulations with minute-by-minute wind speed would result in better agreement between the simulation and the measured data.

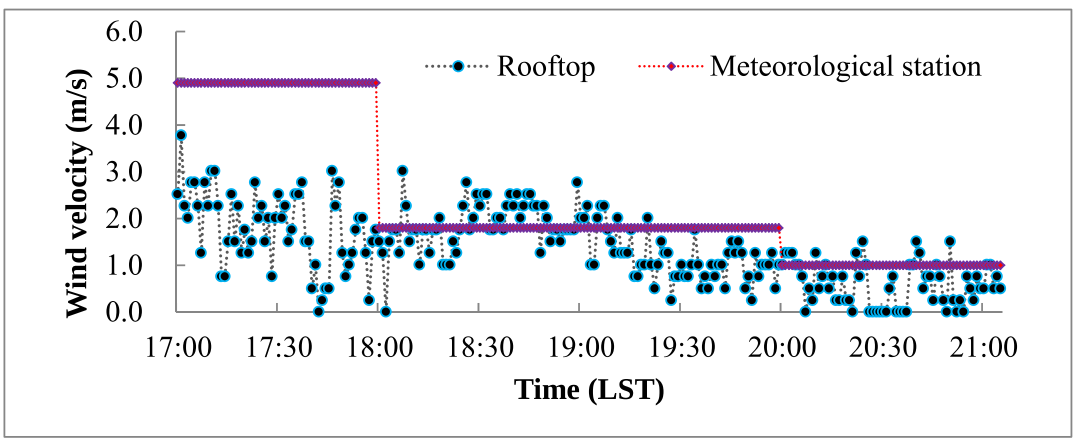

Fig.7. Minute-by-minute wind speed on the building rooftop and hourly wind velocity from the meteorological station from 17:00 to 21:00.

Next, this investigation conducted unsteady CFD simulations by using the modified minute-by-minute meteorological wind information shown in Figure 5 as inflow boundary conditions. Figure 8 compares the simulated wind speed with the measured data on the rooftop of the apartment building. The numerical simulation results agreed well with the measured data. The mean relative error between the numerical results and the experimental data was 24.4%. The error was acceptable for studying airflow around buildings, since there were many uncertainties that could have contributed to this error. This study did not consider the details of the trees around the buildings, but treating them as a roughness length of 0.03 m inside the urban configuration as shown in Fig. 3(a). In addition, there were differences between the geometric model and the actual building structures even inside the urban configuration. Those would cause some errors.

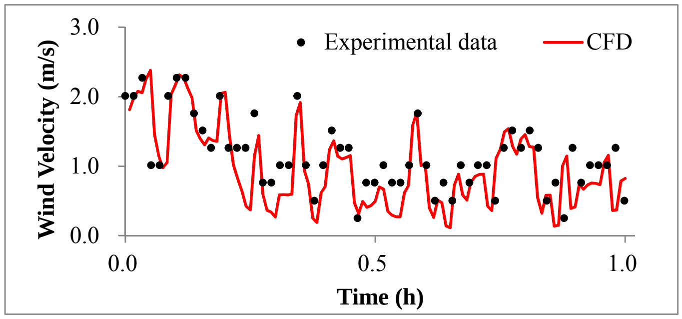

Fig. 8. Comparison of the simulated wind speed with the measured data on the rooftop of the apartment building.

3.3 Calculation of cross-ventilation flow rate

The CFD simulation used in this investigation calculated not only the airflow around the building but also the airflow in the apartment, with the use of the coupled modeling method. At the same time, the simulation determined the CO_2 concentration decay curves in the apartment by using the source information from the measurements. Figure 9 compares the simulated CO_2 concentration decay with the measured data at the five measuring locations in the apartment (as indicated in Figure 2(b)). After 20 minutes, the simulated CO_2 concentration decayed in the same way as that in the experiment. However, there were significant differences within the first 20 minutes.

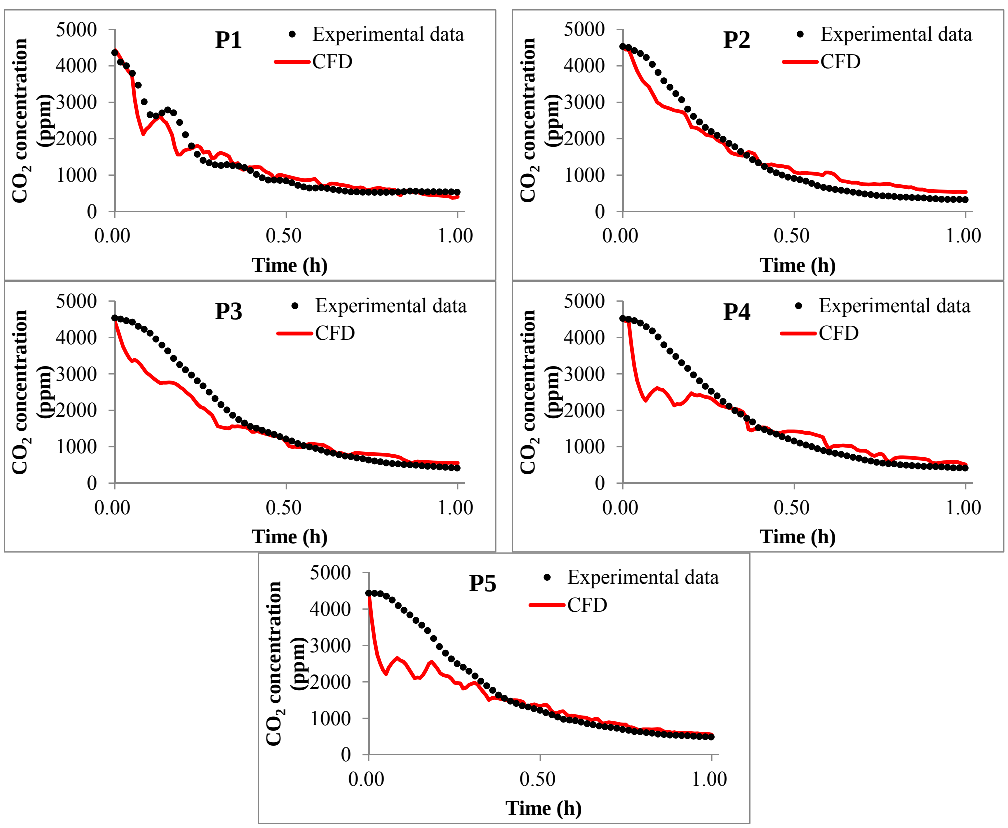

Fig. 9. Comparison between measured and simulated CO_2 concentration decay curves at the five locations in Figure 2(b).

For analysis of the differences, Figure 10 depicts the airflow around the building, the airflow in the apartment, and the indoor CO_2 concentration distribution at a height of 7.9 m above the ground at different time steps, i.e., t = 3, 10, and 20 min. At t = 3 min, the outdoor air flowed into the apartment through the southern window, as shown in the middle section of Figure 10(a). The average air velocity at the south window was 1.1 m/s. The CO_2 concentration decreased considerably in the southern room (bedroom). The right-hand section of Figure 10(a) shows considerable spatial concentration gradients inside the apartment. Since the two exterior windows were located in the separation zones of the approaching wind around the apartment, as shown in the left-hand section of Figure 10(a), the amount of outdoor air entering or leaving the apartment through the windows was very sensitive to the wind direction and speed around the window areas. It is well known that the RNG k-ε model has difficulty in predicting the separations accurately, and the discrepancy between the computed and measured CO_2 concentration was large. Van Hoof et al [46] found that the LES simulation can provide a very good agreement with the experimental data for cross-ventilation rate. However, the use of LES entails an increase in computational demand with a factor of 80 to 100.

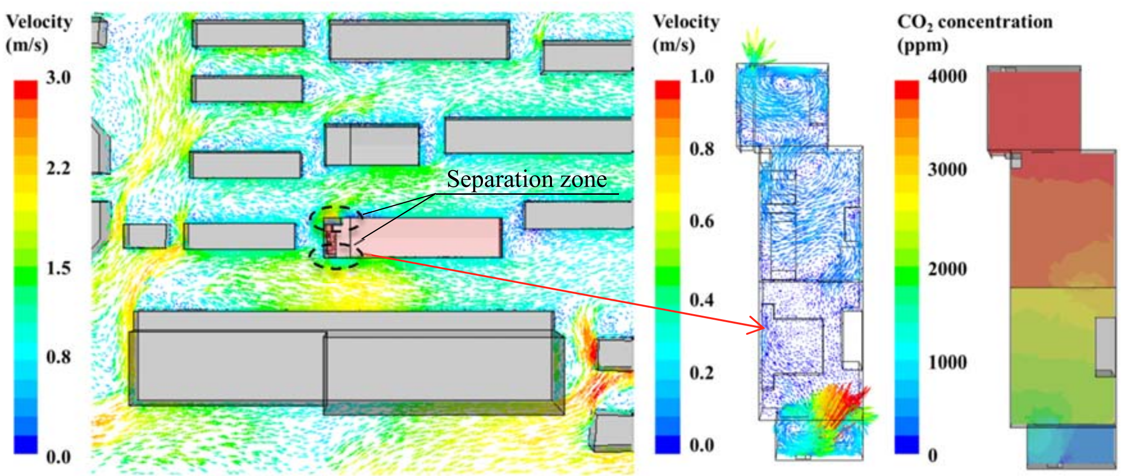

(a) t = 3 min

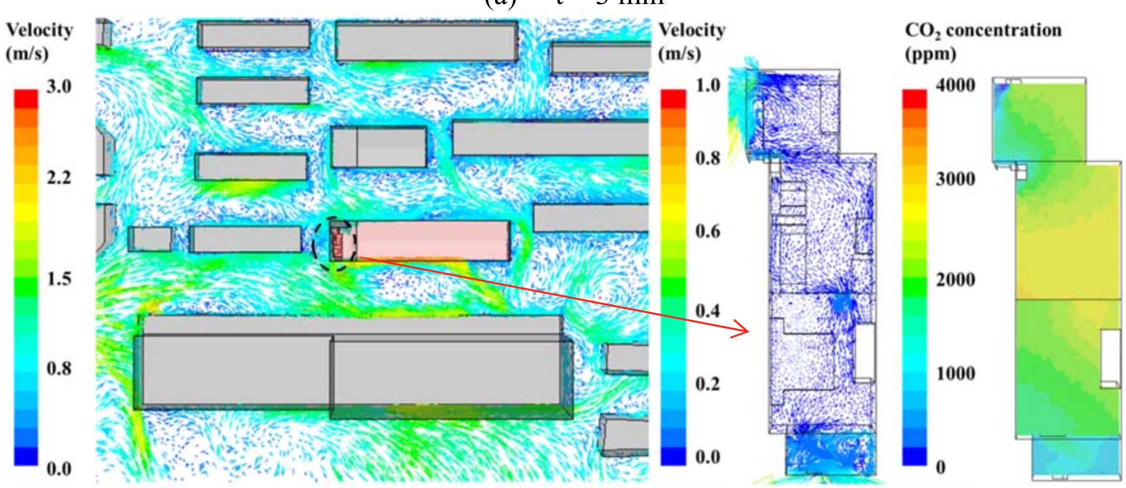

(b) t = 10 min

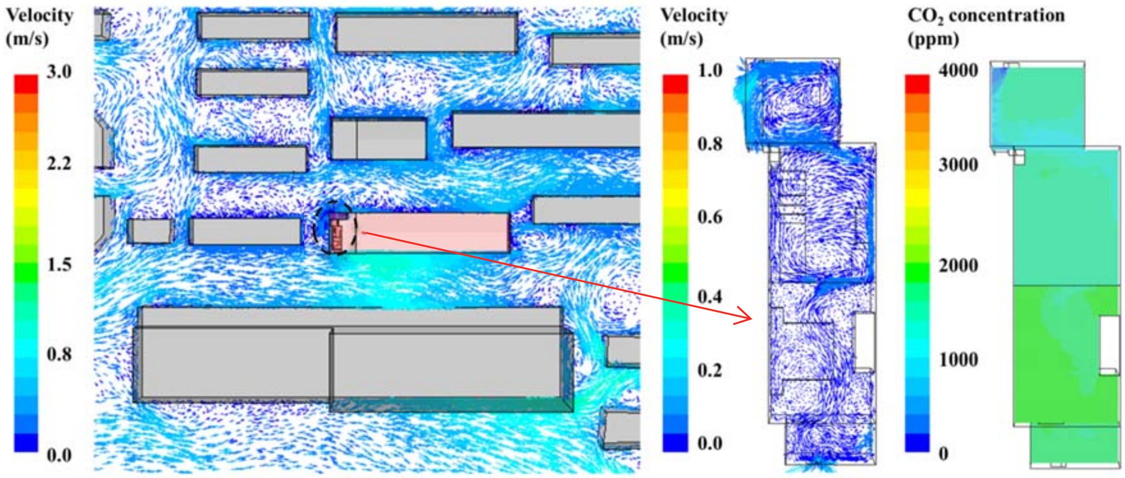

(c) t = 20 min

Fig. 10. Airflow around the building (left), airflow in the apartment (middle), and indoor CO2 concentration distribution (right) at a height of 7.9 m above the ground at different time steps: (a) t = 3 min, (b) t = 10 min, and (c) t = 20 min.

At t = 10 min, the wind speed around the building became lower, as shown in the left-hand section of Figure 10(b). The two separation zones outside the exterior windows disappeared. The average air velocity at the south window was reduced to 0.6 m/s. The CFD simulation should be accurate, and, as a result, it narrowed the difference between the calculated and measured CO_2 concentration in the apartment. Although the wind separation appeared again at t = 20 min, as illustrated in the left-hand section of Figure 10(c), the separation occurred only on the outside of the southern window, and the wind speed was again very low. From t = 20 min to t = 60 min, Figure 8 depicts a low wind speed, and our CFD simulation did not show again the separation on the outside of northern window. Therefore, the predicted CO_2 concentration in the apartment agreed quite well with the measured data.

This investigation further calculated the air change rate in the apartment by using the tracer-gas-decay method [36] with the simulated and measured CO_2 concentrations. Since significant differences existed in the first 20 minutes for the simulated results, this investigation calculated the air change rate through piecewise fitting at different time intervals, i.e., from t = 0 to 20 min, from t = 10 to 20 min, and from t = 20 to 60 min. Figure 11 compares the calculated air change rate with the measured data in the five measurement locations at different time intervals. As expected, from t = 0 to 10 min, CFD calculated a 50% higher air change rate than the measured data because of the two separations of the wind outside the exterior windows of the apartment. From t = 10 to 20 min, CFD under-predicted the air exchange rate in most of the locations in the apartment by an average of 37%. As shown in Figure 8, the predicted wind speed was generally lower than the measured value during this period, which was mainly due to the underestimation of the fluctuations around the building by the RNG k-ε model [47]. The fluctuations reproduced by the model were only by vortex shedding. However, the actual fluctuations comprised a combination of the atmospheric turbulence, building-induced turbulence, and vortex shedding behind the building. Therefore, it may lead to the underestimation of CFD values. The difference was smaller than during the first 10 minutes. From t = 20 to 60 min, the air change rate predicted by CFD was higher than the in the experiment at locations P1, P2, and P3 but lower at P4 and P5. Although the tracer-gas method is effective for measuring the ventilation rate under steady-state conditions, the cross ventilation studied here was not steady. In addition, the CFD prediction still shows the wind separation outside the southern window. Because of the deficiency of the RNG k-ε model and the tracer-gas method, the mean difference between the

CFD result and experiment data during this period was 14% on average, which is acceptable for ventilation design.

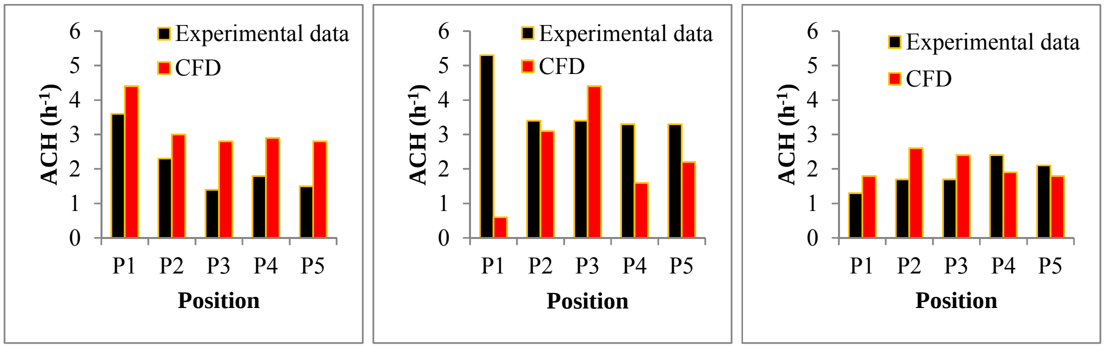

(a) (b) (c)

Fig. 11. Comparison of the CFD-simulated and experimentally determined air change rate at the five locations in the apartment due to cross ventilation, at different time intervals: (a) from t = 0 to 10 min, (b) from t = 10 to 20 min, and (c) from t = 20 to 60 min.

Conventional study of cross ventilation would use steady CFD simulations. According to the results of steady CFD simulation shown in Section 3.2, the corresponding air change rate in the apartment would be 5.3 ACH, calculated as the simulated volumetric flow rate through the apartment (475.2 m^3/h) over the apartment volume (89.2 m^3). The steady CFD simulation significantly overestimated the air change rate, by a factor of two, which is unacceptable.

4. Discussion

Note that this investigation had the following limitations:

- This investigation proposed a method for converting hour-by-hour meteorological data from a meteorological station into minute-by-minute data. However, this method requires that at least one local weather station be installed at the building site of interest. This would increase the cost of a design project, and it may not always feasible. In addition, the proposed method (even if it is using annual data from the meteorological station) would not be able to upscale the process for annual prediction of the ACH which could be very useful for passive design of the buildings.
- This investigation modified the inflow boundary conditions only for the variation in wind speed. However, wind direction is also constantly changing. The relationship between the wind direction from the meteorological station and that on the rooftop of the building may not be simply linear, and should be further investigated.
- This investigation only used wind data from one meteorological station in the upwind direction. In designing natural ventilation, one should consider that the prevailing wind could come from more than one direction. It is essential to study the feasibility of using the same meteorological weather station when it is located in the downstream region of the prevailing wind. This is very important because most medium and small cities in China, for example, have only one meteorological station.
- With the modified minute-by-minute weather data, this investigation used unsteady CFD simulations to simultaneously calculate airflow around a building and airflow in an apartment. For comparison, this investigation also conducted conventional steady CFD simulations. On the same workstation with 24 cores and 128 Gb memory, the computing times for the unsteady and steady simulations were and 58.7 h and 20.6 h,

respectively. The unsteady simulation improved the accuracy but would significantly increase computing costs.

- Because of our limited computing capacity, we only used a time step of 30 s for the unsteady numerical simulations with the RNG k-ε model. A previous study [29] found that time-step size had little influence on the final results. Of course, this applies only to RANS modeling. If the unsteady simulations were performed by means of large-eddy simulations, the time step would be much smaller and the grid resolution would be much finer.
- Most energy simulation programs cannot determine accurate airflow entering a building by natural ventilation, while room air temperature and heating cooling load heavily depend on the airflow. On the other hand, CFD can calculate natural ventilation rate with reasonable accuracy. The combination of CFD and energy simulations can be found in hundreds of papers, such as [48,49]. The modification method proposed could further increase the accuracy of the simulated ACH results.

5. Conclusions

This study performed CFD simulations with the unsteady RNG k-□ model to calculate simultaneously the airflow around a building and the cross-ventilation through an apartment. The method used coupled modeling to perform these simultaneous calculations. The study led to the following conclusions:

- Traditional CFD simulations using constant wind speed do not consider the dynamic wind speed, which may cause errors. This investigation proposed a correlation method to convert hour-by-hour meteorological data from a meteorological station to minute-by-minute data.
- With the modified minute-by-minute data, the variation trend of the wind speed at the rooftop measuring location can be reproduced satisfactorily by the unsteady CFD simulation. The mean relative error between the experimental data and the numerical result was 24.4%.
- When a modified inflow boundary condition is used, the CFD model can predict cross ventilation through the apartment. However, for the specific hour investigated here, the wind generated two separations outside the southern and northern exterior windows. Since the RNG k-ε model could not predict the separation accurately, there were significant difference between the predicted and measured air change rate in the apartment. The use of the tracer-gas method for the unsteady flow contributed further to the difference. Nevertheless, the difference was much smaller than for the conventional steady CFD simulation, which would overestimate the air change rate by a factor of two.

Acknowledgement

The research presented in this paper was partially supported by the National Key R&D Program from the Ministry of Science and Technology, China, on “Green Buildings and Building Industrialization” through Grant No. 2016YFC0700500 and by the National Natural Science Foundation of China through Grant No. 51678395.

References

[1] RMSF Almeida, M Pinto, PG Pinho, LT de Lemos. Natural ventilation and indoor air quality in educational buildings: Experimental assessment and improvement strategies. Energy Efficiency, 10 (2017) 839-854.

[2] Z Tong, Y Chen, A Malkawi, Z Liu, RB Freeman. Energy saving potential of natural ventilation in China: The impact of ambient air pollution. Applied Energy, 179 (2016) 660-668.

[3] RJ de Dear, GS Brager. Thermal comfort in naturally ventilated buildings: Revisions to ASHRAE Standard 55. Energy and Buildings, 34 (2002) 549-561.

[4] TS Larsen. Natural ventilation driven by wind and temperature difference. Aalborg: Department of Civil Engineering, Aalborg University, (2006) (DCE Thesis; No. 2).

[5] H Shetabivash. Investigation of opening position and shape on the natural cross ventilation. Energy and Buildings, 93 (2015) 1-15.

[6] A Aflaki, N Mahyuddin, Z Al-Cheikh Mahmoud, MR Baharum. A review on natural ventilation applications through building faccade components and ventilation openings in tropical climates. Energy and Buildings, 101 (2015) 153-162.

[7] Y Chen, Z Tong, A Malkawi. Investigating natural ventilation potentials across the globe: Regional and climatic variations. Building and Environment, 122(Supplement C) (2017), 386-396.

[8] T van Hooff, B Blocken. On the effect of wind direction and urban surroundings on natural ventilation of a large semi-enclosed stadium. Computers & Fluids, 39 (2010) 1146-1155.

[9] Q Chen. Using computational tools to factor wind into architectural environment design. Energy and Buildings, 36 (2004) 1197-1209.

[10] D Etheridge, M Sandberg. Building ventilation: Theory and measurement. John Wiley and Sons, 1996. p. 93.

[11] C-R Chu, YW Wang. The loss factors of building openings for wind-driven ventilation. Building and Environment, 45(10) (2010), 2273-2279.

[12] RM Aynsley. A resistance approach to estimating airflow through buildings with large openings due to wind. ASHRAE Transactions, 94 (1988) 1661-1669.

[13] T van Hooff, B Blocken, Y Tominaga. On the accuracy of CFD simulations of cross-ventilationflows for a generic isolated building: Comparison of RANS, LES and experiments. Building and Environment, 114 (2017) 148-165.

[14] Y Jiang, D Alexander, H Jenkins, R Arthur, Q Chen. Natural ventilation in buildings: Measurement in a wind tunnel and numerical simulation with large-eddy simulation. Journal of Wind Engineering and Industrial Aerodynamics, 91 (2003) 331-353.

[15] M Shirzadi, M Naghashzadegan, PA Mirzaei. Improving the CFD modelling of cross-ventilation in highly-packed urban areas. Sustainable Cities and Society, 37 (2018) 451-465.

[16] R Ramponia, B Blocken. CFD simulation of cross-ventilation flow for different isolated building configurations: Validation with wind tunnel measurements and analysis of physical and numerical diffusion effects. Journal of Wind Engineering and Industrial Aerodynamics, 104-106 (2012) 408-418.

[17] C-H Hu, T Kurabuchi, M Ohba. Numerical study of cross-ventilation using two-equation RANS turbulence models. International Journal of Ventilation, 4 (2) (2005) 123-131.

[18] Y Jiang, Q Chen. Effect of fluctuating wind direction on cross natural ventilation in buildings from large eddy simulation. Building and Environment, 37 (2002) 379-386.

[19] Z Zhai, SD Hamilton, J Huang, C Allocca, N Kobayashi, Q Chen. Integration of indoor and outdoor airflow study for natural ventilation design using CFD. Proceedings 21st AIVC Annual Conference, “Innovations in Ventilation Technology,” 26-29 September 2000, paper 13.

[20] T van Hooff, B Blocken. Coupled urban wind flow and indoor natural ventilation modelling on a high-resolution grid: A case study for the Amsterdam ArenA stadium. Environmental Modelling & Software, 25 (2010) 51-65.

[21] S Liu, J Liu, Q Yang, J Pei, D Lai, X Cao, J Chao, C Zhou. Coupled simulation of natural ventilation and daylighting for a residential community design. Energy and Buildings, 68 (2014) 686-695.

[22] JI Perén, T van Hooff, BCC. Leite, B Blocken. CFD analysis of cross-ventilation of a generic isolated building with asymmetric opening positions: Impact of roof angle and opening location. Building and Environment, 85 (2015) 263-276.

[23] J Cheng, D Qi, A Katal, LL Wang, T Stathopoulos. Evaluating wind-driven natural ventilation potential for early building design. Journal of Wind Engineering and Industrial Aerodynamics, 182(2018), 160-169.
[24] L Wang, NH Wong. Coupled simulations for naturally ventilated residential buildings. Automation in Construction, 17 (2008) 386-398.
[25] W Wu, B Wang, A Malkawi, N Yoon, Z Sehovic, B Yan. A method toward real-time CFD modeling for natural ventilation. Fluids, 3(4) (2018), 101.
[26] NR Martins, G Carriho da Graça. Validation of numerical simulation tools for wind-driven natural ventilation design. Building Simulation, 9(1) (2016) 75-87.
[27] A Aflaki, K Hirbodi, N Mahyuddin, M Yaghoubi, M Esfandiari. Improving the air change rate in high-rise buildings through a transom ventilation panel: A case study. Building and Environment, 147 (2019) 35-49.
[28] R Zhang, PA Mirzaei, B Jones. Development of a dynamic external CFD and BES coupling framework for application of urban neighbourhoods energy modelling. Building and Environment, 146(2018), 37-49.
[29] T van Hooff, B Blocken. CFD evaluation of natural ventilation of indoor environments by the concentration decay method: CO_2 gas dispersion from a semi-enclosed stadium. Building and Environment, 61(2013) 1-17.
[30] S Liu, W Pan, H Zhang, X Cheng, Z Long, Q Chen. CFD simulations of wind distribution in an urban community with a full-scale geometrical model. Building and Environment, 117(2017) 11-23.
[31] S Liu, W Pan, X Zhao, H Zhang, X Cheng, Z Long, Q Chen. Influence of surrounding buildings on windflow around a building predicted by CFD simulations. Building and Environment, 140 (2018) 1-10.
[32] SM Robaa. Urban-suburban/rural differences over Greater Cairo, Egypt. Atmósfera., 16(2003) 157-171.
[33] ASHRAE. ASHRAE Handbook Fundamentals (SI ed.), ASHRAE, Atlanta, GA (2009).
[34] KS Nikas, N Nikolopoulos, A Nikolopoulos, Numerical study of a naturally cross-ventilated building, Energy Build. 42 (2010) 422-434.
[35] PS, Charlesworth. Air exchange rate and airtightness measurement techniques - An applications guide, Air Infiltration and Ventilation Centre, Coventry, UK; 1988.
[36] X Dai, J Liu, Y Yin, X Song, S Jia. Modeling and controlling indoor formaldehyde concentrations in apartments: On-site investigation in all climate zones of China. Building and Environment, 127(2018) 98-106.
[37] ANSYS Inc.. ANSYS Fluent 14.0 User's Guide. ANSYS Inc. Southpointe. 2011.
[38] TH. Shih, WW. Liou, A. Shabbir, Z. Yang, J. Zhu. A new k-ε eddy-viscosity model for high Reynolds number turbulent flows–Model development and validation. Comput Fluids, 24(3) (1995) 227-38.
[39] GAMBIT CFD Preprocessor. User's Guide. Lebanon, NH: Fluent Inc. 1998.
[40] B Blocken, T Stathopoulos, J Carmeliet. CFD simulation of the atmospheric boundary layer: wall function problems. Atmospheric Environment, 41(2) (2007) 238-52.
[41] BE Launder, DB Spalding. The numerical computation of turbulent flows. Computer Methods in Applied Mechanics Engineering, 3(1974) 269-89.
[42] T Cebeci, P Bradshaw. Momentum transfer in boundary layers. Hemisphere Publishing Corporation, New York, 1977.
[43] J Wieringa. Updating the Davenport roughness classification. Journal of Wind Engineering and Industrial Aerodynamics, 41(1-3) (1992) 357-368.
[44] Y Tominaga, A Mochida, R Yoshie, H Kataoka, T Nozu, M Yoshikawa, T Shirasawa. AIJ guidelines for practical applications of CFD to pedestrian wind environment around buildings. Journal of Wind Engineering and Industrial Aerodynamics, 96 (2008) 1749-1761.
[45] http://data.cma.cn/
[46] V Hooff, B Blocken, Y Tominaga. On the accuracy of CFD simulations of cross-ventilation flows for a generic isolated building: Comparison of RANS, LES and experiments. Building and Environment 114 (2017) 148-165.
[47] Y. Tominaga. Flow around a high-rise building using steady and unsteady RANS CFD: Effect of large-scale fluctuations on the velocity statistics. Journal of Wind Engineering and Industrial Aerodynamics. 142 (2015) 93-103.
[48] W Li, NH Wong. Coupled simulations for naturally ventilated residential buildings. Automation in Construction 17 (2008) 386-398.

[49] Z Zhai, Q Chen, P Haves, JH Klems. On approaches to couple energy simulation and computational fluid dynamics programs. Building and Environment, 37(2002) 857-864.